Electronic Supplementary Material (ESI) for Journal of Materials Chemistry A.
This journal is © The Royal Society of Chemistry 2021

Supporting Information

A mechanically robust and high-wettability multifunctional network binder for high-loading Li-S battery with enhanced rate property

Di Yu,[ab] Qian Zhang,[ac]* Jie Liu,[ab]* Ziyang Guo,[ac] Lei Wang[ad]

[a]*State Key Laboratory base of Eco-chemical Engineering, Taishan Scholar Advantage and Characteristic Discipline Team of Eco-chemical Process and Technology, Qingdao University of Science and Technology, Qingdao 266042, China*

[b]*College of Chemical Engineering, Qingdao University of Science and Technology, Qingdao 266042, China*

[c]*School of Chemistry and Molecular Engineering, Qingdao University of Science and Technology, Qingdao 266042, China*

[d]*College of Environment and Safety Engineering, Qingdao University of Science and Technology, Qingdao 266042, China*

E-mail: q_Zhang2020@126.com (Q. Zhang), jie.liu@qust.edu.cn (J. Liu)

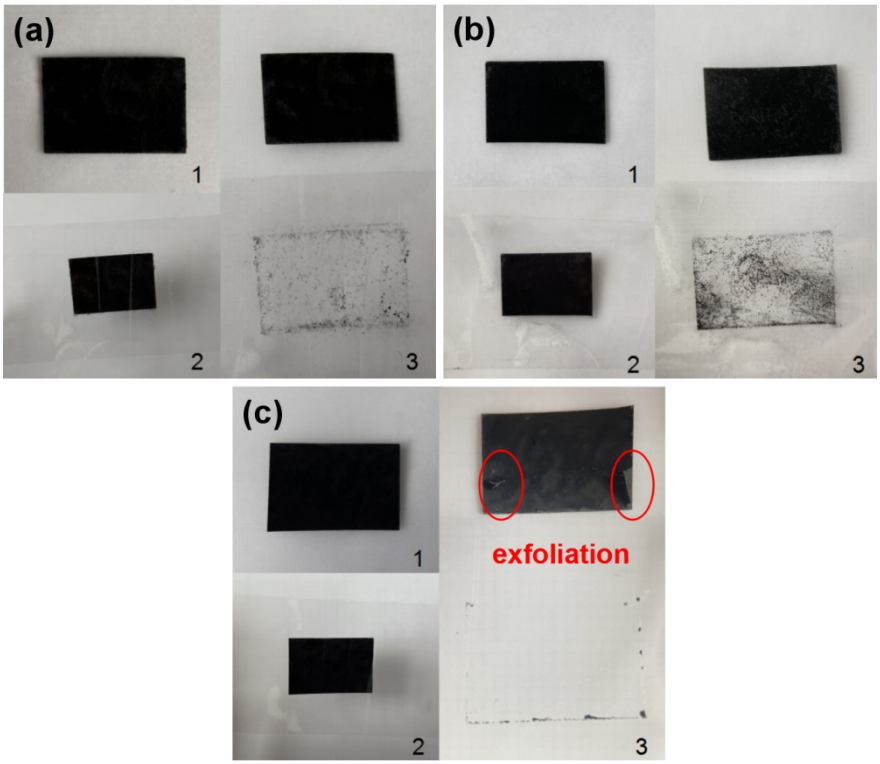

Fig. S1 The peeling tests of the sulfur cathodes with (a) c-Alg-IS binder, (b) Alg binder, and (c) PVDF binder, showing the superior binding capability of c-Alg-IS binder. 1 sulfur cathode after drying; 2 sulfur cathode with adhesive tape; 3 sulfur cathode after peeling off the tape.

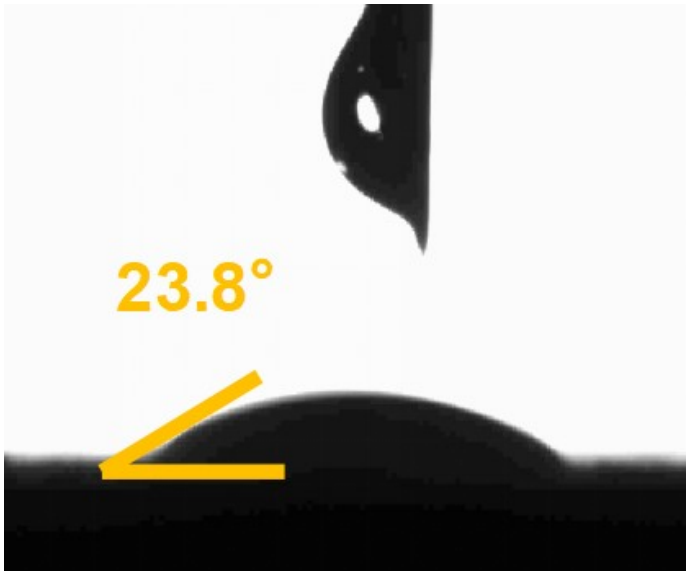

Fig. S2 The electrolyte contact angles of PVDF binder.

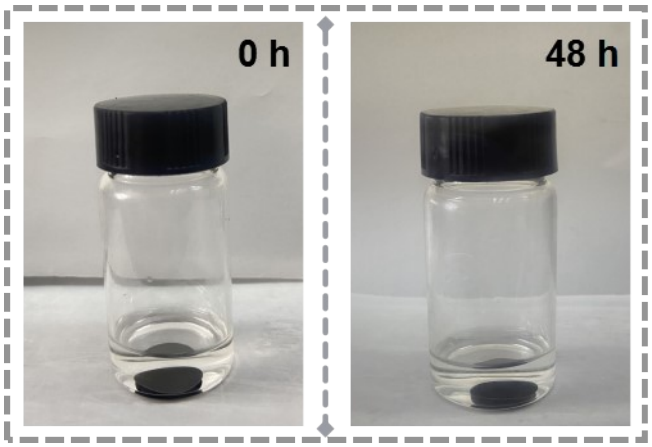

Fig. S3 The digital images of the sulfur cathode using c-Alg-IS binder immersed in the electrolyte of Li-S battery after 0 and 48 h, respectively. The electrode is made of 70 wt% S/super P composite, 10 wt% KB, and 20 wt% c-Alg-IS binder. After soaking for 48 h, the materials are not peeled off from the current collector, which indicates the excellent chemical stability of c-Alg-IS binder in the electrolyte.

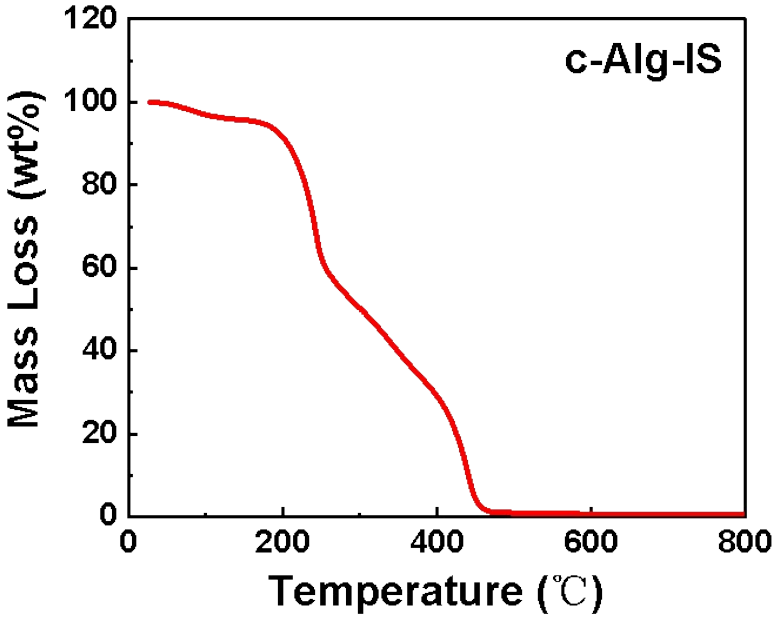

Fig. S4 TGA curve of c-Alg-IS under air flow with a heating rate of 10 ℃ min^{-1}, showing the high thermal stability (up to 200 ℃) of c-Alg-IS under air condition.

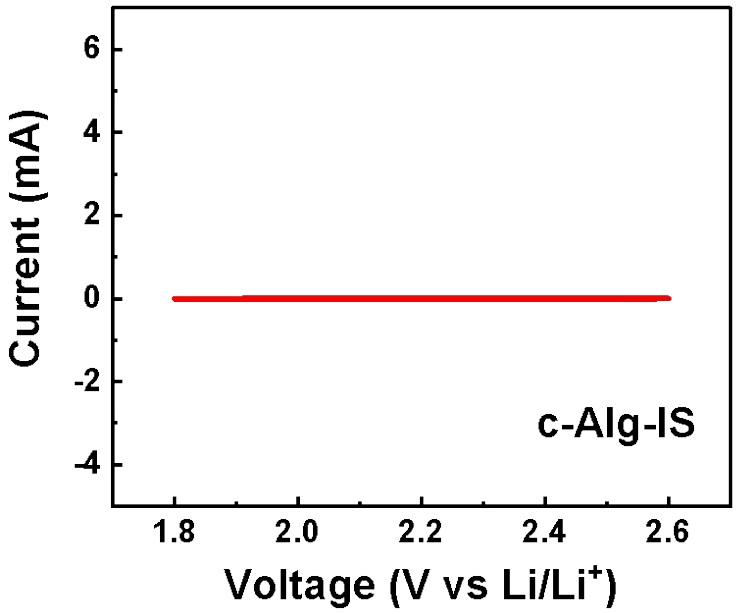

Fig. S5 CV curves of c-Alg-IS binder at 0.1 mV s^{-1}, showing the high electrochemical stability of c-Alg-IS binder.

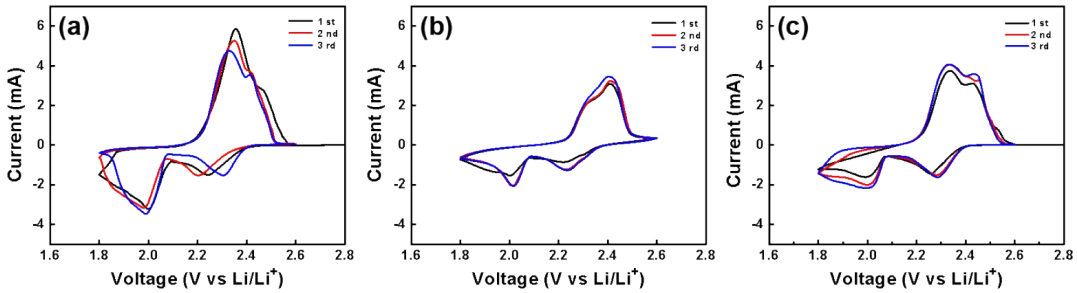

Fig. S6 The CV curves of Li-S cells with (a) Alg, (b) IS, and (c) PVDF binders using a CHI660E electrochemical workstation at a scanning rate of 0.1 mV s^{-1} between 1.8 and 2.6 V.

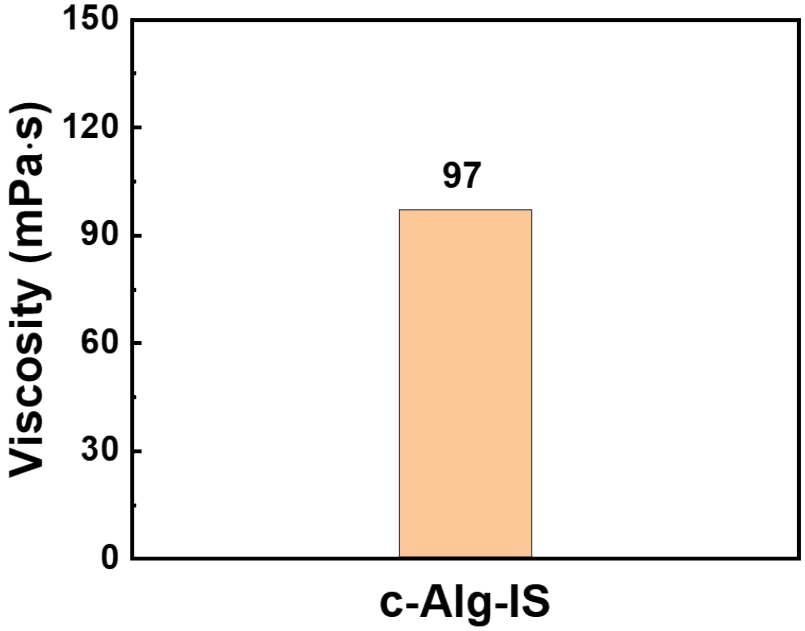

Fig. S7 The viscosity test of IS aqueous solution by rotor 1 on a viscosity analyzer (Techcomp SNP-1).

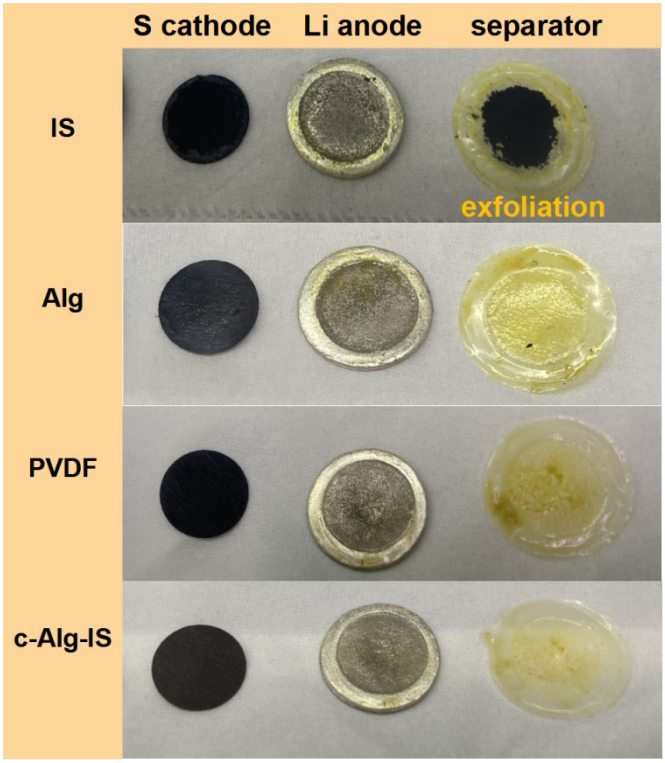

Fig. S8 The digital images of the sulfur cathodes with different binders, Li anodes, and the separators after 20 cycles at 0.2 C.

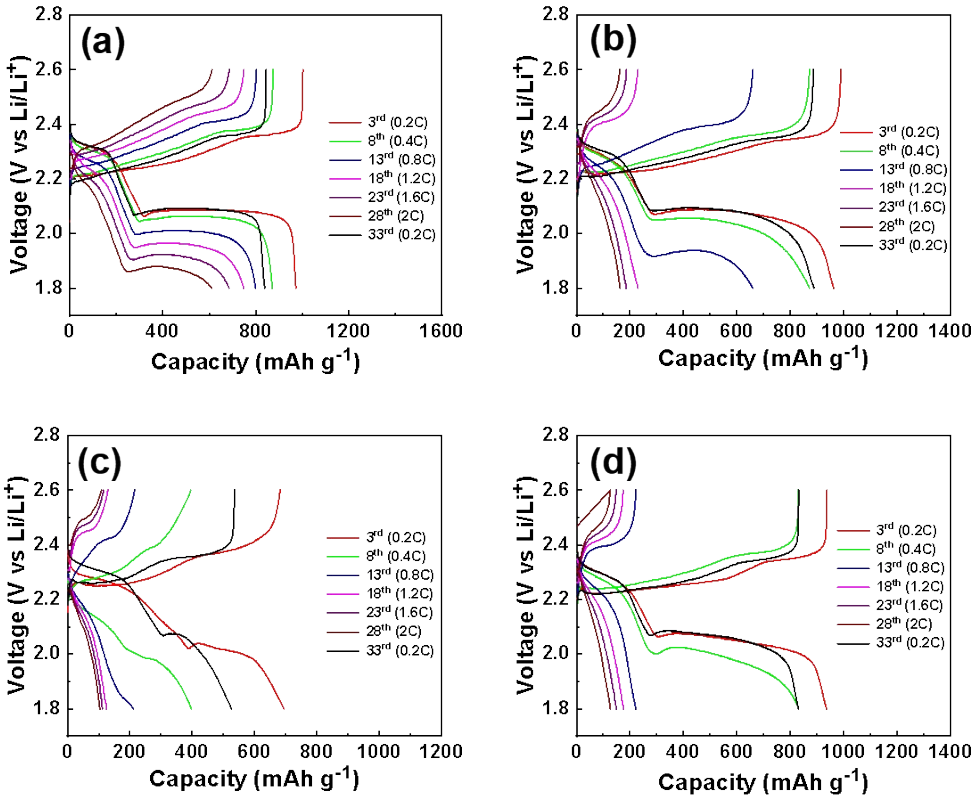

Fig. S9 The charge-discharge curves of Li-S cell with (a) c-Alg-IS, (b) Alg, (c) IS, and (d) PVDF binder at different current rates.

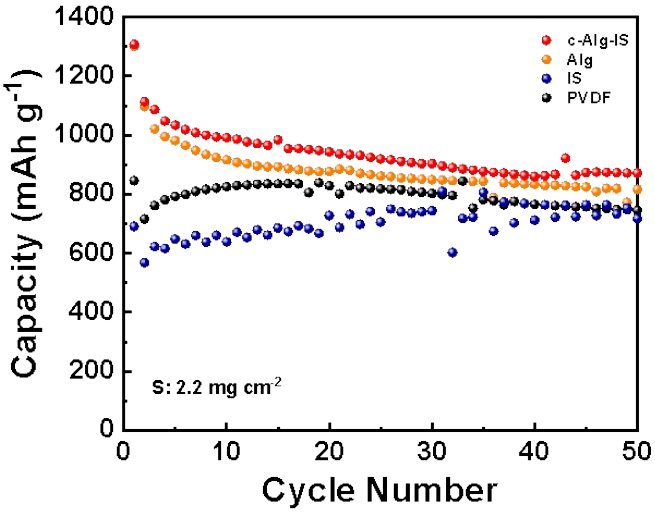

Fig. S10 Comparison of cycling performance of Li-S batteries with different binders at 0.2 C (the first cycle is at 0.1 C). The sulfur cathodes consist of 80 wt% S/super P composite, 10 wt% KB, and 10 wt% binder.

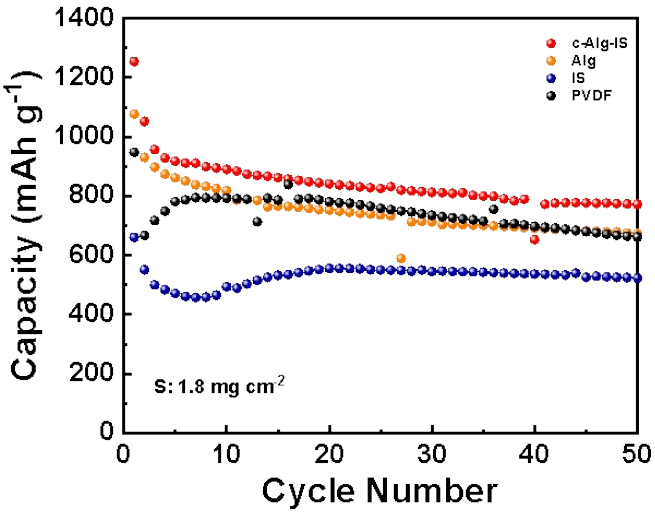

Fig. S11 Comparison of cycling performance of Li-S batteries with different binders at 0.2 C (the first cycle is at 0.1 C). The sulfur cathodes consist of 70 wt% S/super P composite, 10 wt% KB, and 20 wt% binder. The electrolyte is 1M LiTFSI in DOL : DME (1:1 Vol%).

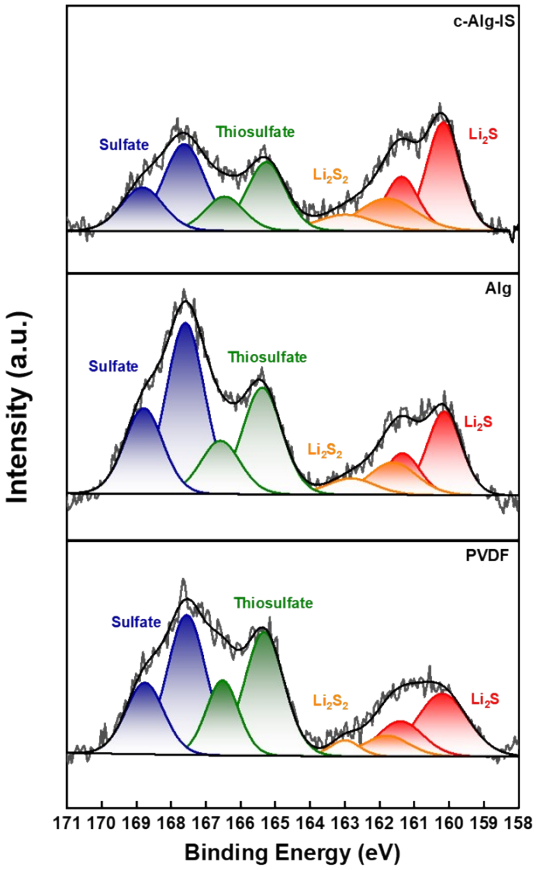

Fig. S12 High-resolution S2p XPS spectra of Li anodes from the Li-S cells using different binders after 20 cycles, showing the sulfide species on the Li anode surfaces are similar.[1,2] The Li anode was cleaned with DME solution before XPS test.

Reference:

1. G. Ye, M. Zhao, L. P. Hou, W. J. Chen, X. Q. Zhang, B. Q. Li, J. Q. Huang, *J. Energy Chem.*, 2022, **66**, 24-29.

2. W. X. Hua, H. Li, C. Pei, J. Y. Xia, Y. F. Sun, C. Zhang, W. Lv, Y. Tao, Y. Jiao, B. S. Zhang, S. Z. Qiao, Y. Wan, Q. H. Yang, *Adv. Mater.*, 2021, https://doi.org/10.1002/adma.202101006.

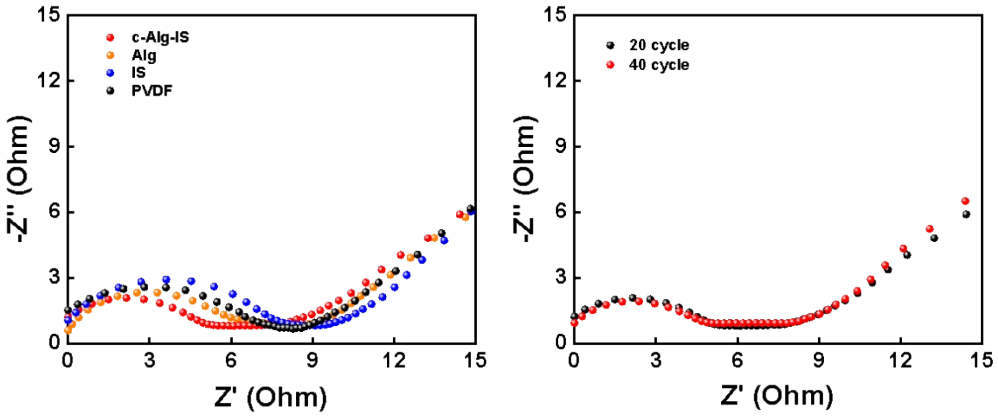

Fig. S13 (a) The Nyquist plots of Li-S batteries with different binders after 20 cycles at 0.2 C; (b) the Nyquist plots of Li-S battery with c-Alg-IS binder after 20 and 40 cycles at 0.2 C.

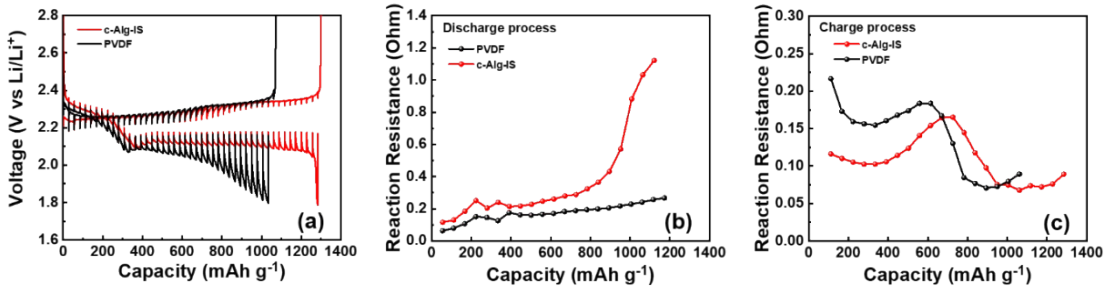

Fig. S14 (a) GITT voltage profiles of Li-S batteries with different binders during the first cycle; reaction resistance comparison of Li-S batteries with different binders (b) during discharge process and (c) during charge process. The galvanostatic intermittent titration technique (GITT) measurements were carried out by applying a pulse constant current of 0.1 C with duration of 10 min, followed by 1 h relaxation to reach an equilibrium voltage. The reaction resistances at different lithiation/delithiation stages were obtained by dividing the overpotential by the pulse current.[1,2]

Reference:

1. K. Xu, X. Liu, J. Liang, J. Cai, K. Zhang, Y. Lu, X. Wu, M. Zhu, Y. Liu, Y. Zhu, G. Wang, Y. Qian, *ACS Energy Letters*, 2018, **3**, 420-427.

2. J. Zhou, X. Liu, L. Zhu, J. Zhou, Y. Guan, L. Chen, S. Niu, J. Cai, D. Sun, Y. Zhu, J. Du, G. Wang, Y. Qian, *Joule*, 2018, **2**, 2681-2693.

Table S1 Comparison of the battery parameters with the recently reported binder-related high-loading Li-S batteries, showing the forefront of our work on areal loading and areal capacity.

Ref.[a]	Polymer binder	Sulfur loading (mg cm^{-2})	Current density	Sulfur content	Initial discharge capacity (mAh g^{-1}) / (mAh cm^{-2})	Reversible discharge capacity (mAh g^{-1}) / Cycle number	Degradation rate per cycle
This work	**c-Alg-IS binder**	**9.1**	**2.4 mA cm^{-2} (~0.16 C)**	**56%**	**1260.2/11.5**	**788.4/60**	**0.62%**
		14.8	**0.4 mA cm^{-2} (~0.02C)**	**56%**	**1198.1/17.8**	**756.3/9**	**NA**
31	SPP binder	8.9	0.1 C	60.61%	932.8/8.3	792.9/50	0.30%
32	S9P1 binder	6.1	0.1 C	60%	999.1/6.1	800.3/50	0.40%
33	SA-Cu binder	8.05	1.0 mA cm^{-2} (~0.07 C)	54%	1180.1/9.5	892.0/29	0.84%
48	PVP/XNBR30 binder	7.0	0.1 C	56%	769.0/5.4	NA	NA
57	G4CMP binder	4.38	0.05C/0.2 C	68%	1045.0/4.32	640.0/100	0.39%
58	PPG binder	4.9	0.1 C	60%	933.6/4.6	761.0/50	0.37%
59	DICP binder	5.5	0.1 C	56%	1448.0/6.39	841.7/100	0.42%
60	PAA-$HPRN^{+}$ binder	6.78	0.1 C	52.16%	1112.1/7.54	1028.0/21	0.36%

[a] The references are listed in the main text.